J Ind Microbiol Biotechnol (2007) 34:363–372
DOI 10.1007/s10295-007-0205-9

ORIGINAL PAPER

A phenomenological model to represent the kinetics of growth by *Corynebacterium glutamicum* for lysine production

Kalyan Gayen · K. V. Venkatesh

Received: 15 September 2006 / Accepted: 29 December 2006 / Published online: 26 January 2007

Abstract *Corynebacterium glutamicum* is commonly used for lysine production. In the last decade, several metabolic engineering approaches have been successfully applied to *C. glutamicum*. However, only few studies have been focused on the kinetics of growth and lysine production. Here, we present a phenomenological model that captures the growth and lysine production during different phases of fermentation at various initial dextrose concentrations. The model invokes control coefficients to capture the dynamics of lysine and trehalose synthesis. The analysis indicated that maximum lysine productivity can be obtained using 72 g/L of initial dextrose concentration in the media, while growth was optimum at 27 g/L of dextrose concentration. The predictive capability was demonstrated through a two-stage fermentation strategy to enhance the productivity of lysine by 1.5 times of the maximum obtained in the batch fermentation. Two-stage fermentation indicated that the kinetic model could be further extended to predict the optimal feeding strategy for fed-batch fermentation.

Keywords Growth kinetics · Structured model · *Corynebacterium glutamicum* · Lysine · Trehalose

K. Gayen · K. V. Venkatesh
Department of Chemical Engineering,
Indian Institute of Technology Bombay, Powai,
Mumbai 400076, India

K. V. Venkatesh (✉)
School of BioSciences and Bioengineering,
Indian Institute of Technology Bombay, Powai,
Mumbai 400076, India
e-mail: venks@che.iitb.ac.in

Introduction

The economic importance of L-lysine demands constant efforts to enhance the productivity through metabolic engineering and optimization of fermentation processes. *Corynebacterium glutamicum* is traditionally used for lysine production [26]. Since genome information of *C. glutamicum* is well known, several metabolic engineering strategies have been attempted to manipulate the biochemistry of this organism for enhancement of lysine production [6, 12, 14, 16, 18]. Moreover, genetic manipulation of lysine producing strain is often approached through inspection of metabolic networks and regulatory mechanisms. Recently, recombinant DNA technology has been employed for productivity [7, 8, 21, 31, 32]. These strategies will help in optimizing the cellular process in the cell to enhance yield of lysine. The optimization of the fermentation process at the reactor level is also equally important for better improvement of both yield and productivity. Past studies suggested that a variety of attempts have been tried to optimize the fermentation processes either by media optimization or by fed batch strategies [3, 9, 11, 19, 20, 22, 24, 25, 30]. The development of a kinetic model is a first step toward bioreactor operation and control. Unfortunately, the kinetics for lysine fermentation using *C. glutamicum* has been neglected. Therefore, the main focus of the current work is to develop a phenomenological model for lysine production.

Modeling the kinetics of the fermentation processes is a challenge to biochemical engineers and biologist. Several kinetic models have been reported for different organisms according to their media composition [1, 4, 5, 10, 29]. The most popular approach, even to

date, is the use of unstructured model such as Monod's model. Unstructured models, however, cannot be able to capture lag phase, regulatory effects and the presence of multiple metabolic paths for substrate uptake [29]. Structured models can address such issues and have better predictive capabilities. For example, lag phase can be predicted by incorporating the synthesis of a key growth enzyme into the kinetics [1, 4, 5]. Cybernetic models extended this idea to capture complex growth processes such as sequential or simultaneous utilization of the substrates by invoking the optimal strategy of the organism toward growth [13, 17]. Recently, this modeling strategy has been employed for representing the kinetics of rifamycin B by *Amycolatopsis mediterranei* in a complex media [2].

Here, we present a phenomenological model to capture the kinetics of lysine production and growth of *C. glutamicum*. We represent the model using three independent paths representing growth, lysine and trehalose production. Parameter values were obtained from batch experiments conducted using different initial dextrose concentrations. The model was able to predict accurately, both batch and two-stage batch operations.

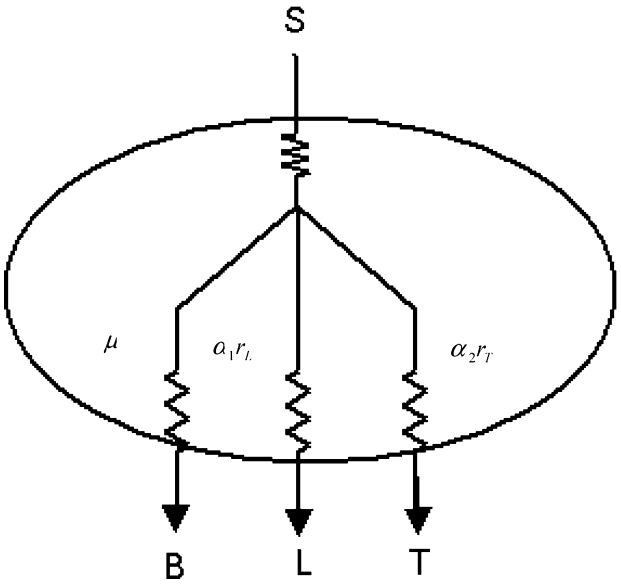

Fig. 1 Schematic representation of the phenomenological model for the growth of *C. glutamicum* on dextrose. Dextrose is effectively consumed through three main paths leading to biomass, lysine and trehalose. It should be noted that the synthesis of lysine and trehalose are regulated and switched on at later stage of fermentation. *S* dextrose; *B* biomass; *L* lysine; *T* trehalose; μ specific growth rate; r_L specific rate for lysine synthesis; r_T specific rate for trehalose synthesis; α_L and α_T control coefficients for lysine and trehalose synthesis, respectively

Model development

The growth of lysine producing strain of *C. glutamicum* on dextrose is associated with the formation of lysine and trehalose. Typically, four phases are observed in the batch growth of *C. glutamicum*. In phase I, balanced exponential growth is observed, which was dependent on the threonine and glucose concentration in the medium. Cell growth continues in the second phase, but is associated with lysine synthesis. In the third phase, lysine synthesis continues while growth decreases. In this phase, trehalose synthesis is also observed. In the last phase, other metabolites such as pyruvate, acetate, lactate, valine, etc. are produced. We present a phenomenological model to represent the three phases of fermentation, as the main objective was to capture the growth and lysine production, which occurs in the first three phases of fermentation. Thus, carbon and nitrogen get distributed into biomass, lysine and trehalose, representing three active metabolic paths during the fermentation. Therefore, three rates can be defined to capture biomass and two products as represented in Fig. 1.

The growth of the organism was observed in the first two phases. The limiting substrates for growth were dextrose and threonine. Therefore, the specific growth rate (μ) is represented as follows:

$$\mu = \mu^{\max} \frac{S}{K_s + S + \frac{S^2}{K_{IS}}} \frac{T_r}{K_{T_r} + T_r} \tag{1}$$

where S is dextrose concentration, T_r is threonine concentration, $\mu^{\max}$ is the maximum specific growth rate, K_S is the dextrose saturation constant, K_{IS} is the dextrose inhibition constant, K_{T_r} is the threonine saturation constant. It is reported that biomass synthesis is strongly related to threonine concentration [27]. Therefore, we assumed that the maximum biomass reached a constant value with the consumption of a fixed amount of threonine. Further, it is reasonable to assume that during the growth phase of the fermentation the value of threonine saturation constant will be very small (i.e., K_{T_r} note that at 0.73 g/L of threonine no limitation was observed). In view of these points, the limitation of threonine can be captured as a logistic function relating to biomass. Therefore, the specific growth rate (μ) can be given as

$$\mu = \mu^{\max} \frac{S}{K_s + S + \frac{S^2}{K_{IS}}} \left(1 - \frac{X}{X^{\max}}\right) \tag{2}$$

where $X^{\max}$ is the maximum biomass produced in a medium for a fixed amount of threonine. It should be

noted that X^{max} is a function of threonine concentration. Here, X^{max} is a constant as we maintain a fixed concentration of threonine for all the experiments. Lysine synthesis occurs in phases II and III. The rate of lysine synthesis (r_L) is given by Eq. 3:

$$r_L = r_L^{max} \frac{S}{K_L + S + \frac{S^2}{K_{IL}}} \tag{3}$$

where, r_L^{max} is the maximum lysine synthesis rate, K_L is the dextrose saturation constant for lysine synthesis and K_{IL} is the dextrose inhibition constant for lysine synthesis. Excess nitrogen was maintained by continuous addition of ammonia into the medium. Thus, ammonium sulfate was not limiting for lysine production. Similarly, trehalose formation rate (r_T) can be represented by Eq. 4:

$$r_T = r_T^{max} \frac{S}{K_T + S + \frac{S^2}{K_{IT}}} \tag{4}$$

where, r_T^{max} is the maximum trehalose synthesis rate, K_T is the dextrose saturation constant for trehalose synthesis and K_{IT} is the dextrose inhibition constant for trehalose synthesis.

It should be noted that lysine and trehalose synthesis do not occur in phase I indicating that cell regulates the synthesis of these products. This implies that both lysine and trehalose synthesis were regulated by the cell. In phase I, typically biomass is optimized by the cellular processes of *C. glutamicum* [23]. Therefore, we define control coefficients, α_L and α_T, which represent the regulation parameters for lysine and trehalose synthesis, respectively. The differential equations capturing the dynamics of biomass formation (X), dextrose consumption (S), lysine (L) and trehalose (T) syntheses are given below:

$$\frac{dX}{dt} = \mu X \tag{5}$$

$$\frac{dL}{dt} = \alpha_1 r_L X \tag{6}$$

$$\frac{dT}{dt} = \alpha_2 r_T X \tag{7}$$

$$-\frac{dS}{dt} = -\frac{1}{Y_{X/S}}\mu X - \frac{1}{Y_{L/S}}\alpha_1 r_L X - \frac{1}{Y_{T/S}}\alpha_2 r_T X \tag{8}$$

where $Y_{X/S}, Y_{L/S}, \text{and} Y_{T/S}$ are the substrate consumption yield coefficients with respect to growth, lysine synthesis and trehalose synthesis, respectively. The model can be extended to predict oxygen consumption and carbon dioxide evolution during fermentation. It is also known that the oxidative phosphorylation is not operating during trehalose formation, since precursor of trehalose is glucose-6-phosphate, which is the first step of glycolysis [27]. This implies that oxygen consumption and carbon dioxide evolution are not related to trehalose synthesis. Equations 9 and 10 show the differential balance for oxygen consumption and carbon dioxide evaluation, respectively,

$$\frac{dCO_2}{dt} = Y_{CO_2/X}\mu X + Y_{CO_2/L}\alpha_1 r_L X \tag{9}$$

$$-\frac{dO_2}{dt} = -Y_{O_2/X}\mu X - Y_{O_2/L}\alpha_1 r_L X \tag{10}$$

where $Y_{CO_2/X}$ and $Y_{CO_2/L}$ are yield coefficient for carbon dioxide evolution with respect to growth and lysine synthesis, respectively. Also, $Y_{O_2/X}$ and $Y_{O_2/L}$ are the oxygen consumption yield coefficient for growth and lysine synthesis, respectively. Equations 1–10 represent the model equations for growth and product formation of *C. glutamicum*.

Materials and methods

Organism and materials

Corynebacterium glutamicum (CECT 79) was obtained from the Spanish Type Culture Collection (CECT), Valencia, Spain and was used in all the experiments. HPLC grade water was purchased form Merck (Mumbai, India). The media (dextrose, tryptone, yeast extract and agar) used for fermentation were purchased form Hi-Media (Mumbai, India). All other chemicals were obtained from sd-fine chemicals (Mumbai, India).

Fermentation protocol

The strain was cultivated and maintained as reported previously [28]. The seed culture was prepared in a medium containing 5 g/L glucose, 5 g/L yeast extract, 10 g/L tryptone and 5 g/L NaCl. One loop of the organism was inoculated from the slant into 250 ml triple baffled conical flask containing 50 ml of seed media. The seed culture was grown for 10 h at 150 rpm maintaining 30°C temperature. Then, 10% (v/v) of seed media was transferred into 500 ml triple baffled round bottom flask containing preculturing media as reported by Vallino [28] and cells were grown for 8 h maintaining the same rpm and temperature. After growing the organism in the preculturing medium, the culture was

transferred into the fermentation medium. Fermentation was initiated by inoculating the fermentation medium [28] with 10% v/v precultured seed. All the fermentations were carried out in laboratory bioreactor with working volume of 1.5 L (BIOSTAT B plus, Sartorius, Goettingen, Germany). Airflow rate was controlled at 1 L/min/L of the reactor volume. The stirrer speed of the fermentor was kept at 1,000 rpm throughout the experiment. pH was maintained at 7.0 by feeding ammonia via peristaltic pump. All the fermentation experiments were performed in duplicate and the data was reported as an average. The maximum deviation for concentrations of dextrose, biomass and trehalose around the average was about 3%, whereas a maximum deviation of 8% was observed for lysine.

Online measurements

Online measurements were performed through data acquisition software supplied by Sartorius (Goettingen, Germany). Temperature, airflow rate, dissolved oxygen, pH and cumulative ammonia addition were monitored during the experiment. Off gas (oxygen uptake rate and carbon dioxide evolution rate) was also monitored by an off gas analyzer (Emerson process management, Germany).

Off line measurements

Samples were drawn in regular intervals during the course of fermentation for analysis of dry cell weight, glucose, trehalose, lysine and ammonium sulfate. Dry cell weight was estimated using spectrophotometer (V-540, Jasco, Tokyo, Japan) with the absorbance at 600 nm. One unit of absorbance was equivalent to 0.28 g/L of dry cell weight. Glucose and trehalose were estimated using RI detector in HPLC (Hitachi, Merck, KgaA, Darmstndt, Germany) with a HP-Aminex-87-H column (Biorad, Inc., Hercules, CA) at 60°C. The mobile phase in HPLC was 5 mM sulfuric acid and the flow rate was maintained at 0.6 mL/min. The concentration of lysine was measured by HPTLC method as reported by Pachuski et al. [15]. Ammonium sulfate was measured using ion analyzer (EA940 Ion analyzer, Thermo Orion, Beverly, MA).

Results and discussion

Batch experiments were conducted with varying initial dextrose concentrations of 17, 27, 57, 95, 117 and 138 g/L with a fixed threonine concentration of 0.73 g/L. The model equations contain a total of 16 parameter values including three maximum rate of formations (μ^{max}, r_L^{max} and r_T^{max}), three saturation constants (K_S, K_L and K_T), three inhibition constants (K_{IS}, K_{IL} and K_{IT}) and seven yield coefficients ($Y_{X/S}, Y_{L/S}, Y_{T/S}, Y_{CO_2/X}, Y_{CO_2/L}, Y_{O_2/X}, Y_{O_2/L}$). It should be noted that the two control coefficients (α_L and α_T) are variables, which need to be dynamically evaluated to solve the differential equations. The values of these control coefficients were obtained based on the phenomenological observation of lysine and trehalose synthesis. These were evaluated using the following inequalities:

$$\alpha_L = 0 \quad \text{if} \quad \frac{X}{X^{max}} \leqslant f_L \quad \text{and} \quad \alpha_L = 1 \quad \text{if} \quad \frac{X}{X^{max}} > f_L \tag{11}$$

$$\alpha_T = 0 \quad \text{if} \quad \frac{X}{X^{max}} \leqslant f_T \quad \text{and} \quad \alpha_T = 1 \quad \text{if} \quad \frac{X}{X^{max}} > f_T \tag{12}$$

where, f_L or f_T represents the ratio of biomass concentration with the maximum biomass formed (X^{max}). The above inequality ensures that in phase I (i.e., $0 \leqslant f \leqslant f_L$), only growth occurs, while lysine and trehalose synthesis would be absent. Further, phase II and III are represented by the range of fractional biomass given as $f_L < f \leqslant f_T$ and $f_T < f \leqslant 1$. The yield coefficients were evaluated from experimental consumption rates of substrates and accumulation rates of products. The other model parameters were estimated using the set of data obtained form various initial dextrose concentrations by least square method. Further, the parameters were fine-tuned using dynamic optimization algorithm ''fimincon'' available in MATLAB (Mathworks, Natick, MA, USA). It can be noted that the values of f_L and f_T were 0.73 and 0.93, respectively.

Table 1 shows the values of 16 parameters used in the model. A high maximum specific growth rate (0.58/h) was observed, which was dependent on the concentration of threonine used. Further, maximum specific lysine synthesis rate was half that of the specific growth rate, while maximum lysine synthesis rate was approximately fivefold higher than that of trehalose synthesis rate. The dextrose saturation constant for growth (K_S) was eightfold less than that for lysine synthesis (K_L) and the dextrose saturation constant for lysine synthesis (K_L) was twofold less than that for trehalose synthesis (K_T). Interestingly, a reverse trend was observed for the dextrose inhibition constant. The dextrose inhibition constant for growth (K_{IS}) was approximately double that for lysine synthesis (K_{IL}) and the inhibition constant for lysine (K_{IL}) was 0.5-fold greater than that for trehalose (K_{IT}). In summary, all the three parameters indicate that the organism prefers

Table 1 Model parameters for growth and products formation using the strain *Corynebacterium glutamicum* (CECT 79)

μ^{max} (h^{-1})	0.58	K_{IT} (g/L)	61
K_S (g/L)	1.5	$Y_{X/S}$(g/g)	0.76
$K_{I\,S}$ (g/L)	150	$Y_{L/S}$ (g/g)	0.38
r_L^{max} (h^{-1})	0.29	$Y_{T/S}$ (g/g)	0.5
K_L (g/L)	12.3	$Y_{CO_2/L}$ (g/g)	0.72
$K_{I\,L}$ (g/L)	84	$Y_{CO_2/X}$ (g/g)	0.93
r_T^{max} (h^{-1})	0.06	$Y_{O_2/L}$ (g/g)	0.75
K_T (g/L)	25	$Y_{O_2/X}$ (g/g)	0.74

μ^{max} maximum specific growth rate; K_S dextrose saturation constant for growth; K_{IS} dextrose inhibition constant for growth; r_L^{max} maximum lysine synthesis rate; K_L dextrose saturation constant for lysine synthesis; K_{IL} dextrose inhibition constant for lysine synthesis; r_T^{max} maximum trehalose synthesis rate; K_T dextrose saturation constant for trehalose synthesis; K_{IT} dextrose inhibition constant for trehalose synthesis; $Y_{X/S}$, $Y_{L/S}$ and $Y_{T/S}$ are the substrate consumption yield coefficients with respect to growth, lysine synthesis and trehalose synthesis; Y_{CO_2}/X and Y_{CO_2}/L are yield coefficient for carbon dioxide evolution with respect to growth and lysine synthesis; Y_{O_2}/X and Y_{O_2}/L are the oxygen consumption yield coefficient for growth and lysine synthesis

to consume dextrose for growth, with high specific growth rate, low saturation constant and high inhibition constant. Also, it prefers production of lysine over trehalose. The yield coefficient for oxygen consumption was almost same for both growth and lysine synthesis, while for carbon dioxide evolution the yield coefficient for biomass was larger compared to the lysine synthesis. This is reflected due to higher flux in TCA cycle during cell growth as compared to lysine synthesis phase.

The parameter values were used to solve the kinetic model represented by Eqs. 2–12. Figure 2a shows the model fit with experimental data for the growth of *C. glutamicum* on 27 g/L of initial dextrose concentration. The model was able to represent the data accurately. In this case, about 11.5 g/L of biomass and only 3.7 g/L of lysine were formed with negligible amount of trehalose. This implies that effectively only phases I and II were observed for growth on 27 g/L of initial dextrose concentration. Figure 2b shows the model fit for the case when cells were grown on 52 g/L of initial dextrose concentration. In this case, dextrose was completely consumed by 17 h yielding 15 g/L of biomass, 11 g/L of lysine and 1 g/L of trehalose. Figure 2c shows the model fit for the case when cells were grown on 95 g/L of initial dextrose. In this case, biomass concentration was also 15 g/L with lysine and trehalose concentration being 18 and 7 g/L, respectively. It should be noted that the amount of biomass formed (15 g/L) was the same for growth on media containing 52 and 95 g/L, indicating that threonine was not limiting for growth below 52 g/L. Further, the model was able to capture the different phases observed during lysine fermentation.

A batch run containing 72 g/L of initial dextrose concentration was conducted to capture the model prediction. It should be noted that the data for growth on 72 g/L of dextrose was not used for parameter estimation. Figure 3a shows the match of the prediction with experimental data and it is clear that the model was able to accurately predict the profiles. In this case, about 18 g/L of lysine was formed with 15 g/L of biomass and 2.1 g/L of trehalose. The dependence of threonine concentration on the formation of maximum biomass can be verified as the same X^{max} was observed beyond 52 g/L of initial dextrose in the media. The model was also used to determine the carbon dioxide evaluation and oxygen consumption in the fermentation (Fig. 3b). It can be observed that the model was able to predict the dynamics until 18 h, beyond which the prediction and the experimental data deviated. The region of deviation (beyond 18 h) represents phase IV of the fermentation, where other metabolites (e.g., alanine, valine, pyruvate, acetate, etc.) accumulate. This phase was not incorporated in the model. Figure 3c shows the variation of control coefficients (α_L and α_T) at various points for the media containing 72 g/L of dextrose. Phase I extended till 8.3 h, phase II was between 8.3 and 9.4 h and phase III was between 9.4 and 18 h. Figure 3c also shows the variation of control coefficients (α_L and α_T) at various time points for the medium containing 27 and 95 g/L of glucose. It is clear that α_L and α_T values were highly dependent on the initial dextrose concentration. At higher dextrose concentration due to substrate inhibition, the phases shifted to the right indicating that more time was taken to switch on lysine synthesis. It can be seen that for 27 g/L of dextrose, phase II was for 1.0 h extending from 7.25 to 8.25 h, whereas for 95 g/L, phase II was for 1.7 h from 9.1 to 10.8 h.

Figure 4a shows model prediction of the rates of biomass, lysine and trehalose synthesis for the case of medium containing 72 g/L of initial dextrose concentration. The biomass synthesis rate occurred until 21 h, while lysine synthesis rate extended from 8.3 to 23 h with trehalose synthesis rate between 9.4 and 22 h. Also, the maximum productivity was observed for lysine synthesis with a value of 2.1 g/L at 15 h than for biomass (1.5 g/L at 8 h) and trehalose formation rate was the lowest. This indicates that the cells excrete lysine due to excess carbon flux, which was not balanced by growth alone. Further, maximum rate of growth and product formation decreases with decrease in initial substrate concentration and decreases also for higher initial concentration (data not shown). This

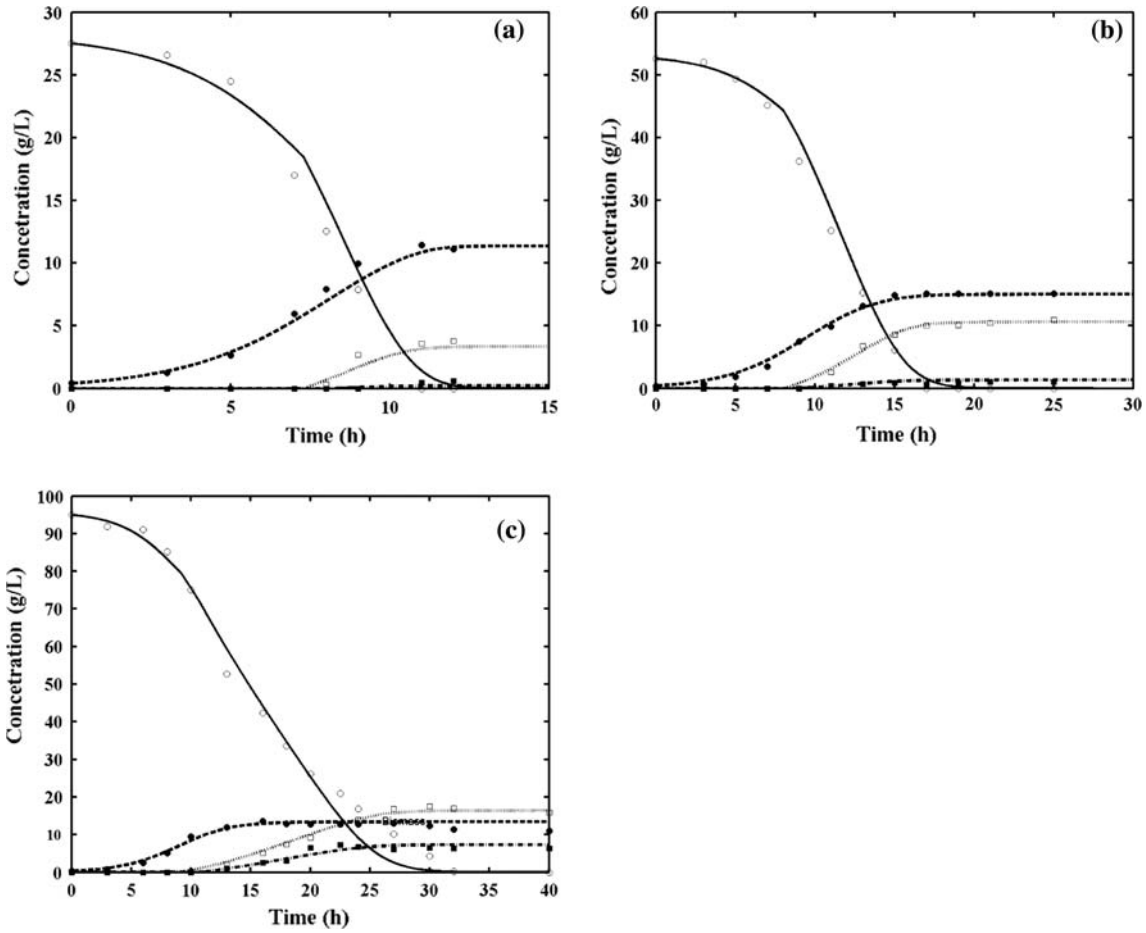

Fig. 2 Model comparison with experimental data of substrate consumption and product formation profiles for the fermentation of *C. glutamicum* for different initial dextrose concentrations. *Symbols* indicate experimental values: *open circle* dextrose; *filled circle* biomass; *open square* lysine; *filled square* trehalose. *Lines* indicate the model prediction: *solid line* dextrose; *dash line* biomass; *dotted line* lysine; *dash-dotted line* trehalose. Initial dextrose concentration of 27 g/L (**a**), 52 g/L (**b**) and 95 g/L (**c**)

indicated that the initial dextrose concentration of about 72 g/L was optimum with respect to lysine formation rate. Figure 4b shows the consumption rate of dextrose and oxygen and evolution rate of carbon dioxide. In this case, the three profiles run almost parallel. The rate of glucose consumption was the highest among all the metabolites with a maximum rate of 7 g/Lh at 14 h, representing phase III of fermentation. Since all the three metabolic paths were active, the dextrose uptake rate was high in this phase.

Batch experiments with various dextrose concentrations for a fixed threonine concentration of 0.73 g/L demonstrated a constant $X^{\max}$ of 15 g/L. A total of 72 g/L of dextrose yielded the optimum lysine concentration of 18 g/L. A batch experiment with 150 g/L of dextrose in the medium yielded 15 g/L of biomass, 18 g/L of lysine and 7 g/L of trehalose. This implied that at high concentration of dextrose, fixed concentration of threonine yielded similar biomass and lysine concentration, channeling the excess carbon toward other metabolites. Therefore, the model was used to predict the fermentation profile when dextrose and threonine were supplemented into the media containing 72 g/L of glucose and 0.73 g/L of threonine just after the lysine synthesis began at 11 h. Concentrated dextrose and threonine were added at 11 h resulting in an excess of 72 and 0.73 g/L, respectively, in the media. It should be noted that there was almost negligible dilution of other components. The model predicted that the lysine and trehalose synthesis will be high using such an addition of excess dextrose and threonine during the batch fermentation. The biomass concentration reached 29 g/L as shown in Fig. 5a. The availability of excess dextrose in the presence of increased biomass enhanced the lysine productivity to 30 g/L. The model prediction matched the data obtained by experiments accurately. The fermentation time was 25 h as compared to about 60 h for the

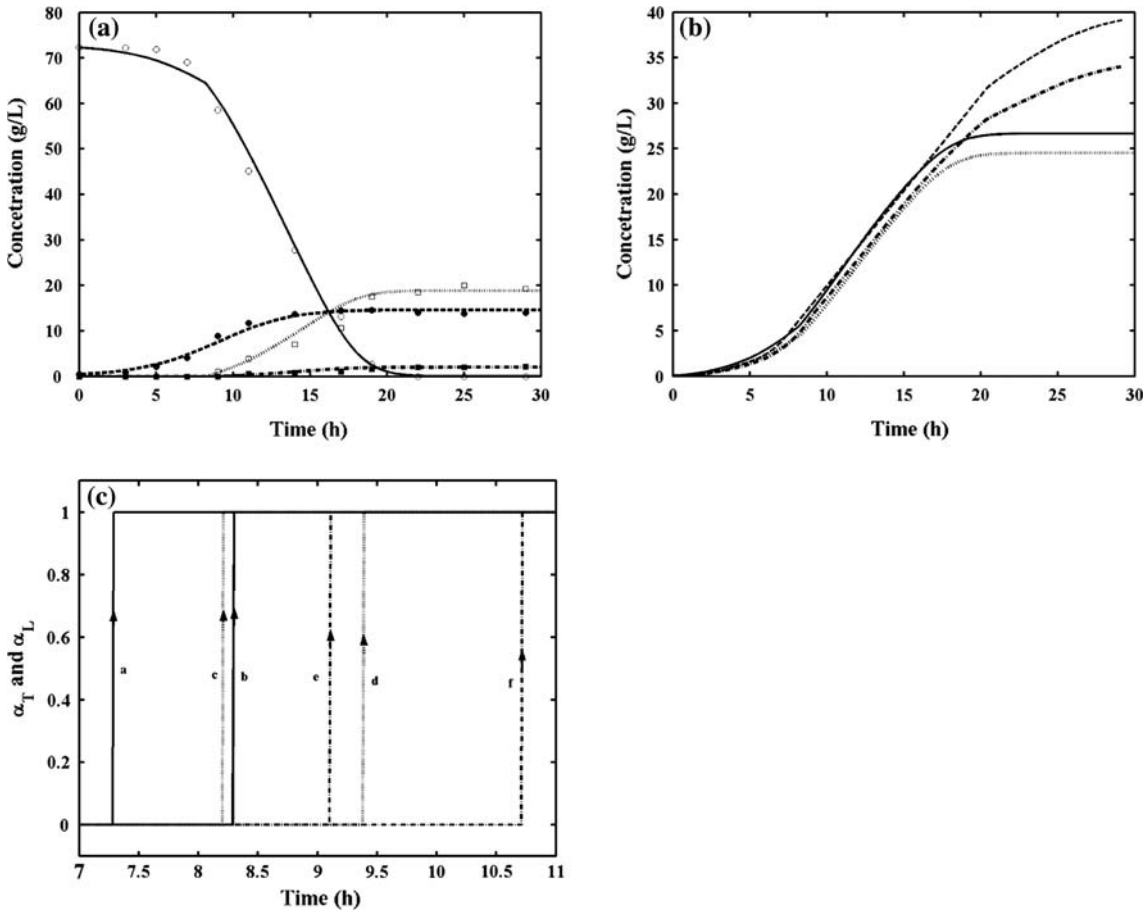

Fig. 3 Comparison of model prediction with experimental data for growth of *C. glutamicum* on 72 g/L of initial dextrose. **a** Profiles of dextrose, biomass, lysine and trehalose. *Symbols* indicate experimental values: *open circle* dextrose; *filled circle* biomass; *open square* lysine; *filled square* trehalose. *Lines* indicate the model prediction: *solid line* dextrose; *dash line* biomass; *dotted line* lysine; *dash-dotted line* trehalose. **b** Profiles of net amount of oxygen consumed and carbon dioxide formed. *Dash line* and *dash-dotted line* represent the experimental concentration values of carbon dioxide and oxygen, respectively; *solid line* and *dotted line* represent the simulated values of carbon dioxide and oxygen, respectively. **c** Dynamic responses of control coefficients (α_L and α_T) for different initial dextrose concentrations (27, 72 and 95 g/L) during the course of fermentation. *a*, *c* and *e* represent the switching on of α_L for 27, 72 and 95 g/L of initial glucose concentrations, respectively; *b*, *d* and *f* represent the switching on of α_T for 27, 72 and 95 g/L of initial glucose concentrations, respectively

batch with 150 g/L of dextrose in the medium. Figure 5b shows the predicted values of control coefficient (α_L and α_T). The control coefficient for lysine (α_L) switched on at 8 h, but on addition of excess substrate at 11 h, it attained a value of zero immediately. After 12 h, the value of α_L again rose to unity indicating that lysine synthesis had restarted. Similar trend was also observed for the other control coefficient (α_T). It should be noted that the net $X^{\max}$ was double as excess threonine was introduced at $t = 11$ h. This also had an effect on lysine productivity due to increase biomass concentration. Further, substrate inhibition on all the three specific rates (μ, r_L and r_T) was avoided due to serial addition of substrate in a two-stage type operation.

Table 2 summarizes the productivity of biomass, lysine and trehalose at various initial dextrose concentrations along with their fermentation time. It is clear from the table that the fermentation times increase with increase in initial substrate concentration. The effect of substrate inhibition was visible beyond initial dextrose concentration of 72 g/L. The maximum biomass productivity was at initial dextrose concentration of 27 g/L, in which case minimum productivities of lysine and trehalose were observed. In this case, 73% of total product formation was toward biomass and only 23 and 4% were toward lysine and trehalose, respectively. Maximum lysine productivity was observed at 72 g/L of dextrose, while maximum trehalose productivity was observed at 95 g/L of dextrose. At

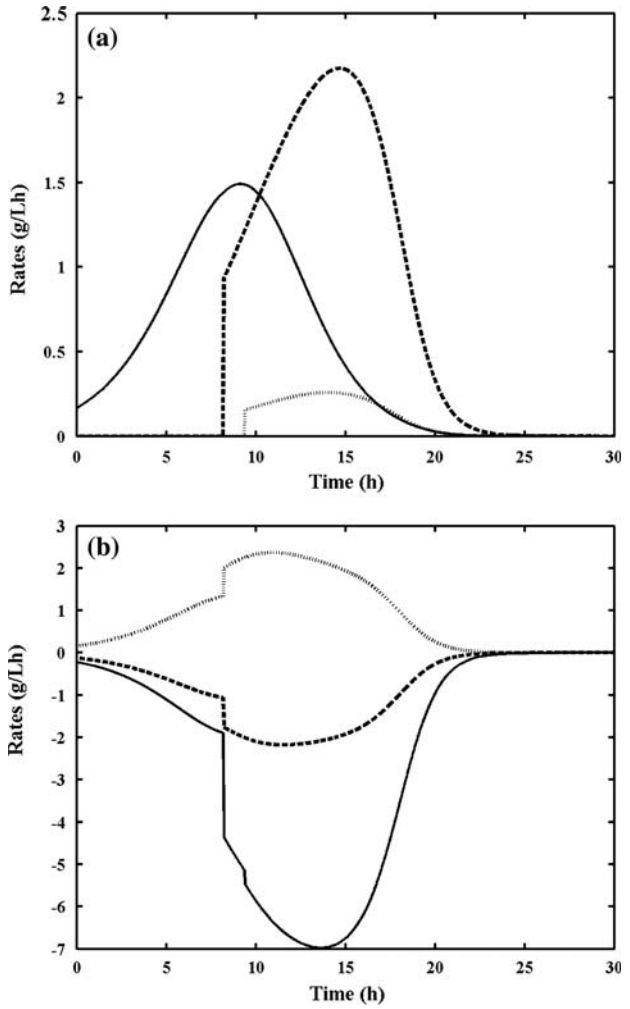

Fig. 4 Model prediction of growth rate, oxygen consumption rate and products formation rate for the growth of *C. glutamicum* on 72 g/L of initial dextrose concentration. **a** *Solid line* indicates rate of biomass formation, *dash line* indicates lysine synthesis rate and *dotted line* indicates trehalose synthesis rate. **b** *Solid line* indicates dextrose consumption rate, *dash line* indicates oxygen consumption rate and *dotted line* indicates carbon dioxide evolution rate

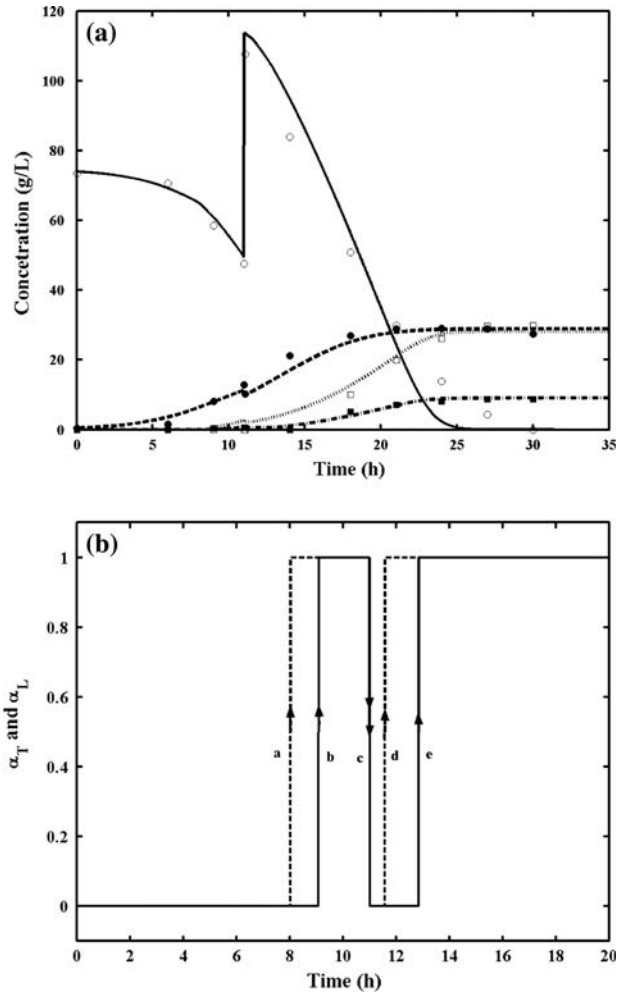

Fig. 5 Model prediction and comparison with experimental data for growth of *C. glutamicum* on 72 g/L of initial dextrose, supplemented with an equvalent glucose and threonine at 11.0 h in two stage fermentation **a** Profiles for dextrose, biomass, lysine and trehalose. *Symbols* indicate experimental values: *open circle* dextrose; *filled circle* biomass; *open square* lysine; *filled square* trehalose. *Lines* indicate the model prediction: *solid line* dextrose; *dash line* biomass; *dotted line* lysine; *dash-dotted line* trehalose. **b** Responses of control coefficients (α_L and α_T) during the course of fermentation. *a* and *b* represent the switching on of α_L and α_T respectively. *c* represents the switching off of both the control coefficients at the start of the second stage. *d* and *e* represent re-switching on of α_L and α_T, respectively in the second-stage

72 g/L, 43, 50 and 7% of the total product formation were toward biomass, lysine and trehalose, respectively, while at 95 g/L, 38, 45 and 17% were toward biomass, lysine and trehalose, respectively. It can be noted that the sum of the three product formation was highest at 72 g/L of dextrose. The substrate limitation reduces the net product toward the three products below 72 g/L, while accumulation of other metabolites decreased the net productivity above 72 g/L of dextrose. Addition of 72 g/L in two-stages, resulted in maximum net productivity of 2.7 g/Lh (i.e., for all the three products), of which 43, 44 and 13% were toward biomass, lysine and trehalose, respectively. This indicates that a fed batch operation would be the best mode of operation for lysine production. In summary, *C. glutamicum* prefers to channel carbon toward growth at lower dextrose concentration. When excess carbon was available in the media, the organism still prefers to channel carbon toward biomass; the extra carbon was channeled first to lysine and then to trehalose. It should be noted that this hierarchy of product formation was also observed through the parameter values that were used in the model.

Table 2 Batch productivity (g/Lh) for fermentation of biomass, lysine and trehalose for different initial dextrose concentration and two-stage fermentation

S_0 (g/L)	t_F (h)	Biomass (g/Lh)	Lysine (g/Lh)	Trehalose (g/Lh)
17	8	0.93	0.0	0.0
27	12	0.94	0.31	0.05
52	17	0.88	0.65	0.06
72	21	0.71	0.83	0.12
95	30	0.50	0.60	0.23
117	40	0.38	0.45	0.18
138	60	0.25	0.30	0.12
Two stage (72 + 72)	25	1.16	1.20	0.34

The fermentation time (t_F), the time taken to completely consume dextrose, is also reported

Conclusions

A kinetic model was developed to capture the dynamics of growth and product formation for lysine synthesis using *C. glutamicum*. The phenomenological model was able to capture the effects of various dextrose concentrations on growth and synthesis of lysine and trehalose. The model incorporated the switching on of the product synthesis during fermentation using control coefficients. Experiments indicated that 72 g/L of initial dextrose concentration was optimum for lysine production, while 95 g/L yielded maximum trehalose. The model was able to accurately predict a two-stage batch fermentation wherein 144 g/L of dextrose was added in two-stages. Thus, the predictive capability of the model was demonstrated. The model can be further used to develop optimal feeding strategies for fed batch operation.

Acknowledgements The authors are thankful to Mr. Navneet Rai for his assistance in conducting experiments. KVV acknowledges financial support for the research from Swarnajayanti fellowship, Department of Science and Technology, India.

References

1. Bajpai-Dikshit J, Suresh AK, Venkatesh KV (2003) An optimal model for representing the kinetics of growth and product formation by Lactobacillus rhamnosus on multiple substrates. J Biosci Bioeng 96:481–486
2. Bapat PM, Bhartiya S, Venkatesh KV, Wangikar PP (2006) Structured kinetic model to represent the utilization of multiple substrates in complex media during rifamycin B fermentation. Biotechnol Bioeng 93:779–790
3. Coello N, Brito L, Nonus M (2000) Biosynthesis of L-lysine by *Corynebacterium glutamicum* grown on fish silage. Bioresource Technol 73:221–225
4. Doshi P, Rengaswamy R, Venkatesh KV (1997) Modelling of microbial growth for sequential utilization in a multisubstrate environment. Process Biochem 32:643–650
5. Doshi P, Venkatesh KV (1998) An optimal model for microbial growth in a multiple substrate environment: simultaneous and sequential utilization. Process Biochem 33:663–670
6. Eggeling L, Sahm H (1999) L-Glutamate and L-lysine: traditional products with impetuous developments. Appl Microbiol Biotechnol 52:146–153
7. Eikmanns BJ, Eggeling L, Sahm H (1993) Molecular aspects of lysine, threonine, and isoleucine biosynthesis in *Corynebacterium glutamicum*. Antonie van Leeuwenhoek 64:145–163
8. Follettie MT, Sinskey AJ (1986) Recombinant DNA technology for *Corynebacterium glutamicum*. Food Technol 40:88–93
9. Kiefer P, Heinzle E, Wittmann C (2002) Influence of glucose, fructose and sucrose as carbon sources on kinetics and stoichiometry of lysine production by *Corynebacterium glutamicum*. J Ind Micro Biotechnol 28:338–343
10. Lendenmann U, Egli T (1998) Kinetic models for the growth of *Escherichia coli* with mixtures of sugars under carbon-limited conditions. Biotechnol Bioeng 59:99–107
11. Manfred K, Pfefferle W (2001) The fermentative production of L-lysine as an animal feed additive. Chemosphere 43:27–31
12. Mockel B, Marx A, Hermann T, Farwick M, Pfefferle W (1999) Bedeutung und Potential des Corynebacterium glutamicum ATCC 13032-Genomprojekts. Transkript 10–11, 41–42
13. Narang A, Konopka A, Ramkrishna D (1997) Dynamic analysis of the cybernetic model for diauxic growth. Chem Eng Sci 52:2567–2578
14. Ohnishi J, Mitsuhashi S, Hayashi M, Ando S, Yokoi H, Ochiai K, Ikeda M (2002) A novel methodology employing *Corynebacterium glutamicum* genome information to generate a new L-lysine-producing mutant. Appl Microbiol Biotechnol 58:217–223
15. Pachuski J, Fried B, Sherma J (2002) HPTLC analysis of amino acids in *Biomphalaria Glabrata* infected with *Schistosoma mansoni*. J Liq Chromatogr Relat Technol 25:2345–2349
16. Pfefferle W, Mockel B, Bathe B, Marx A (2003) Biotechnological manufacture of lysine. In: Faurie R, Thommel J (eds) Advances in biochemical engineering/biotechnology. Microbial production of L-amino acids, vol 79. Springer, Berlin, pp 59–112
17. Ramakrishna R, Ramkrishna D, Konopka AE (1997) Microbial growth on substitutable substrates: characterizing the consumer–resource relationship. Biotechnol Bioeng 54:77–90
18. Sahm H, Eggeling L, Eikmanns B, Kramer R (1995) Metabolic design in amino acid producing bacterium *Corynebacterium glutamicum*. FEMS Microbiol Rev 16:243–252
19. Sassi AH, Deschamps AM, Lebeault JM (1996) Process analysis of L-lysine fermentation with *Colynebacterium glutamicum* under different oxygen and carbon dioxide supplies and redox potentials I. Process Biochem 31:493–497
20. Sassi AH, Fauvart L, Deschamps AM, Lebeault JM (1998) Fed-batch production of L-lysine by *Corynebacterium glutamicum*. Biochem Eng J 1:85–90
21. Schwarzer A, Pithier A (1990) Genetic manipulation of the amino acid-producing *Corynebacterium glutamicum* strain ATCC 13032 by gene disruption and gene replacement. Biomed Tech 9:84–87
22. Seibold G, Auchter M, Berens S, Kalinowski J, Bernhard JE (2006) Utilization of soluble starch by a recombinant *Corynebacterium glutamicum* strain: growth and lysine production. J Biotechnol (in press)

23. Stephanopoulos G, Vallino J (1991) Network rigidity and metabolic engineering in metabolite overproduction. Science 252:1675–1681
24. Stewart J, Niven JDB, Peter HB (2006) The effect of controlled fermentation on the fate of synthetic lysine in liquid diets for pigs. Anim Feed Sci Technol (in press)
25. Takiguchi N, Fukui N, Shimizu N, Shimizu H, Shioya S (1998) Method of *Corynebacterium glutamicum* fermentation time extension with high lysine production rate by leucine addition. J Ferment Bioeng 86:180–184
26. Tryfona T, Bustard MT (2005) Fermentative production of lysine by *Corynebacterium glutamicum*: transmembrane transport and metabolic flux analysis. Pocess Biochem 40:499–508
27. Vallino JJ (1991) Identification of branch-point restrictions in microbial metabolism through metabolic flux balance analysis and local network perturbations. Ph. D. Thesis, Massachusetts Institute of Technology, USA
28. Vallino JJ, Stephanopoulos G (1991) Metabolic flux distributions in *Corynebacterium glutamicum* during growth and lysine over-production. Biotechnol Bioeng 41:633–646
29. Venkatesh KV, Doshi P, Rengaswamy R (1997) An optimal strategy to model microbial growth in a multiple substrate environment. Biotechnol Bioeng 56:635–644
30. Yang C, Hua Q, Shimizu K (1999) Development of a kinetic model for L-lysine biosynthesis in *Corynebacterium glutamicum* and its application to metabolic control analysis. J Biosci Bioeng 88:393–403
31. Yeh P, Sicard AM, Sinskey AJ (1988) General organization of the genes specifically involved in the diaminopimelatelysine biosynthetic pathway of *Corynebacterium glutamicum*. Mol Gen Genet 212:105–111
32. Yoshihama M, Higashiro K, Rao EA, Akedo M, Shanabrruch WG, Follettie MT, Walker GC, Sinskey AJ (1985) Cloning vector system for *Corynebacterium glutamicum*. J Bacteriol 62:591–597